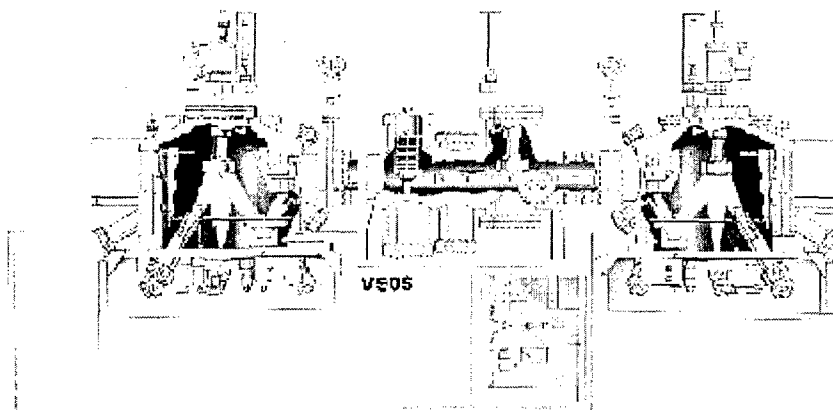


| REPORT DOCUMENTATION PAGE   |             |  |   |   |
|---|-------------|--|---|---|
| <small>The public reporting burden for this collection of information is estimated to average 1 hour per response, including the time for reviewing and maintaining the data needed, and completing and reviewing the collection of information. Send comments regarding this burden estimate or any other aspect of this collection of information, including suggestions for reducing the burden, to Department of Defense, Washington Headquarters Services, Directorate for Information Operations and Reports, 1215 Jefferson Davis Highway, Suite 1204, Arlington, VA 22202-4302. Respondents should be aware that notwithstanding any other provision of law, no person shall be subject to any penalty for failing to comply with a collection of information if it does not display a currently valid OMB control number.</small><br><b>PLEASE DO NOT RETURN YOUR FORM TO THE ABOVE ADDRESS.</b> |             |  |   |   |
| 1. REPORT DATE (DD-MM-YYYY)<br>26-05-2006   |             | 2. REPORT TYPE<br>Final Technical Report |   | 3. DATES COVERED (From - To)<br>7/1/2005 to 1/31/2006     |
| 4. TITLE AND SUBTITLE<br>Hybrid Mole Computer Using Vapor Phase Assembly  |             |  | 5a. CONTRACT NUMBER                             |   |
|   |             |  | 5b. GRANT NUMBER<br>FA9950-05-1-0423            |   |
|   |             |  | 5c. PROGRAM ELEMENT NUMBER                      |   |
| 6. AUTHOR(S)<br>Harriott, LR, Bean, JC, Stan, M, Swami, N.  |             |  | 5d. PROJECT NUMBER                              |   |
|   |             |  | 5e. TASK NUMBER                                 |   |
|   |             |  | 5f. WORK UNIT NUMBER                            |   |
| 7. PERFORMING ORGANIZATION NAME(S) AND ADDRESS(ES)<br>University of Virginia  |             |  | 8. PERFORMING ORGANIZATION<br>REPORT NUMBER     |   |
| 9. SPONSORING/MONITORING AGENCY NAME(S) AND ADDRESS(ES)<br>USAF, AFRL<br>AF Office of Scientific Research<br>875 N. Randolph St. Rm3112<br>Arlington, VA 22203<br>Dr. Anne Marsuam AFSOR/NE 200c.marsuam@afsor.af.mil   |             |  | 10. SPONSOR/MONITOR'S ACRONYM(S)<br>AFSOR/DARPA |   |
|   |             |  | 11. SPONSOR/MONITOR'S REPORT<br>NUMBER(S)       |   |
| 12. DISTRIBUTION/AVAILABILITY STATEMENT<br><i>Distribution Statement A: unlimited</i>   |             |  |   |   |
| 13. SUPPLEMENTARY NOTES   |             |  |   |   |
| 14. ABSTRACT<br>The International Technology Roadmap for Semiconductor (ITRS) has been updated recently to recognize these difficulties and lists emerging device technologies for the future which promise to allow continued improvement in micro- and nan-electronics. One of the technologies cited in the most recent ITRS is molecular electronics. The advantages of molecular devices are based on the fact that the electrically active molecules are inherently small and can be chemically tailored for various functionalities. At the University of Virginia, we have a research program in this area. A particular focus for our program is materials and process compatibility of molecular devices with conventional CMOS electronics in a hybrid architecture.   |             |  |   |   |
| 16. SUBJECT TERMS<br>molecular electronics, nanoelectronics   |             |  |   |   |
| 16. SECURITY CLASSIFICATION OF:   |             |  | 17. LIMITATION OF<br>ABSTRACT                   | 18. NUMBER<br>OF<br>PAGES                                 |
| a. REPORT   | b. ABSTRACT | c. THIS PAGE                             |   |   |
|   |             |  |   | 19a. NAME OF RESPONSIBLE PERSON<br>Lloyd R. Harriott      |
|   |             |  |   | 19b. TELEPHONE NUMBER (include area code)<br>434-243-5580 |

**Final Technical Report: Hybrid Mole Computer Using Vapor Phase Assembly**  
**FA9550-05-1-0423**

The UHV vapor phase assembly of molecules was performed in a stainless steel chamber that is part of a molecular beam epitaxy (MBE) system (shown on the following page) that Professor John Bean brought to the University of Virginia from Bell Labs. This MBE system has two chambers: one that was used for silicon and germanium growth, and the second (referred to as Dep 2 from now on) we engineered for the vapor phase deposition of organic molecules.



**Figure 1.1:** The Molecular Beam epitaxy chambers at the University of Virginia, Dep 2 is the left chamber and Dep 1 is the right chamber.

This entire section is dedicated to describing the changes that had to be made to Dep 2 in order to use it for the vapor phase deposition of organic molecules. The changes to the chamber included adding: a turbo molecular

**DISTRIBUTION STATEMENT A**  
Approved for Public Release  
Distribution Unlimited

**20060614023**

---

pump that would not get clogged with molecules, heaters to keep the gauges from becoming contaminated with molecules, a source for the vaporization of the liquid alkanethiols, and a special low temperature thermal cell to vaporize the powder oligo(phenylene ethynylene) (OPE) and diazo molecules. Additionally, to purify both the liquid and powder molecules prior to vaporization, we built two different purification stations that are also described in this section.

## A Molecule Compatible Pumping System

In order to maintain an ultra-high vacuum system, we required pumps that could pump down to and maintain pressures of approximately  $1 \times 10^{-8}$  mbar. Prior to our work with Dep 2, it maintained UHV pressures using a cryogenic (cryo) pump. This is a pump that removes gas from the chamber by creating an extremely cold surface (a carbon adsorber) on which the gaseous molecules condense<sup>1</sup>. Overtime, the adsorber "fills up" with condensed gas and can be regenerated by being slowly heated up to room temperature. As the pump reaches room temperature, the condensed molecules return to the gas phase and then vent into the atmosphere.

There were several problems with using a cryo pump for a chamber that would be used for the vaporization of organic molecules. Although the pump might have initially worked during the molecular vaporization, as the molecules vaporized they would have condensed on the filter inside of the pump. Over time, the pump adsorber would have filled with molecules and needed to be

---

regenerated. Because the molecules that we used for vapor phase assembly were liquids or solids at room temperature and were known for their self-assembling properties, room temperature regeneration may not have been adequate. Also, the vaporization temperatures of some of the molecules used were as high as 150°C, but the cryo pump could only sustain temperatures up to 100°C. Thus, even with heating the pump up to its temperature limit, regeneration would probably not have removed all of the molecules from the filter of the pump.

Another problem with using a cryo pump on Dep 2 for molecular vaporization is that during regeneration the pump is typically vented out to the room. However, some of the self-assembling molecules used in this work have an EXRTEMLY pungent odor (similar to that of skunk spray) and there is even some question as to whether these molecules are carcinogenic with long-term exposure. Thus, even if we could get all of the molecules out of the pump during regeneration, the pump could not be safely vented into the room.

For these reasons, we decided to switch the pump on Dep 2 to a turbo molecular pump. This "turbo" pump has fan-like blades that collide with the gas entering the pump and "push" it out the exhaust side of the pump<sup>1</sup>. This pump would have advantages over the cryo pump in that it does not "store" the gas (molecules) and that it could be exhausted through a line to the outside of the building. In choosing a turbo pump, we decided on the Pfeiffer 1601 pump with

---




a Pfeiffer DCU 600 display unit. The position of the turbo pump on the chamber is shown in Figure 1.2 (1).

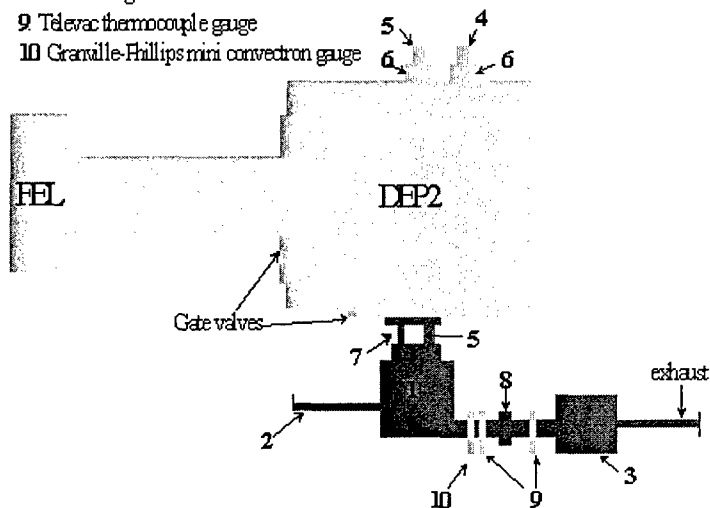
In addition to price, this pump was chosen because it had a throughput rate of 750 cubic centimeters per minute and the ability for the operator to vary its operation speed. The throughput rate is the volume of gas pumped per minute and needed to be high enough to achieve and maintain ultra-high vacuum pressures. The ability for the operators to vary the turbo speed was a desired feature because it gave us the option of doing higher-pressure vaporizations. This feature could be used for the in-situ evaporation of metal for contacting molecular monolayers. Decreasing the energy of the incoming metal atoms should result in fewer destroyed devices because the top metal would be less likely to penetrate through the molecular monolayer. This feature of the pump has not yet been used, but may be used in the future.

We also ordered some additional features and accessories for the Pfeiffer 1601 turbo pump. One of these was a valve that allowed for nitrogen gas to be purged over the turbo pump bearings during operation (Figure 1.2 (2)). This purging gas was to keep the molecules from attaching to the bearings and clogging the pump. We also ordered a heating jacket for the pump that could heat the pump to 275°C (Pfeiffer PM 041 913-T), so that if any molecules did attach inside the pump we could heat it to vaporize them back out. Because the operation of the turbo pump required a backing pump, we ordered a Pfeiffer Duo 020MC corrosive rotary vein pump (Figure 1.2 (3)). This pump is an oil free

pump, which eliminates the chance of oil from this pump contaminating the turbo pump and/or the chamber. This pump removed the exhaust from the turbo pump and then was exhausted outside of the building. Each of these pumps can be seen in the Figure 1.2

- 1: Pfeiffer 1601 turbo pump
- 2 Nitrogen line for venting and purging turbo pump
- 3 Pfeiffer 020MC rotary vane pump
- 4 Pfeiffer IKR 060 cold cathode gauge
- 5 Pfeiffer TPR 018 penani gauge
- 6 Watlowband heaters
- 7 nipple (for drawings see Appendix 3)
- 8 Pfeiffer angle valve
- 9 Televac thermocouple gauge
- 10 Granville-Phillips mini convection gauge

-  = existing equipment
-  = pumping equipment added
-  = gauges added



---

Figure 1.2: Diagram showing the back of the Dep 2 system including pumps and gauges that were added for molecular vaporization capabilities.

## 5.1 Molecule-Safe Pressure Gauges

In order for the pressure to be determined at various parts of the system, pressure gauges were installed. A standard type of pressure gauge used to measure ultrahigh vacuum pressures is the ion gauge (Bayert-Alpert gauge). This gauge measures the number of gas molecules in a chamber by ionizing the gas with electrons and then collecting these ions on a charged plate and measuring the charge<sup>1</sup>. For a "hot filament" gauge, these electrons are "boiled" out of a filament that is heated white hot (i.e. 2000 °C). However, we did not want any hot filaments in the system with the molecules because we feared that some molecules could get into the gauges, interact with the hot filaments, chemically decay, and then contaminate the samples with unknown decayed molecules. Thus, for the main vacuum chamber measurement we used a cold cathode gauge (Pfeiffer IKR 060, see in Figure 1.2 (4)). This gauge is similar to a hot cathode gauge, but emits electrons via a voltage potential<sup>1</sup>, rather than using a hot filament. The cold cathode gauge can measure down to  $5 \times 10^{-10}$  mbar, but only operates at pressures below  $1 \times 10^{-2}$  mbar.

---

In order to measure pressures from atmosphere to below  $10^{-2}$  mbar, we also purchased a Pfeiffer pirani gauge model TPR 018 (Figure 1.2 (5)). This pirani gauge is composed of a mildly heated resistor inside of a tube and works using the principle that the lower the pressure, the less heat can be conducted between the tube filament and the tube wall through convection. As the pressure in the tube drops, the convection heat flow between the gauge filament and the tube wall will decrease. As the temperature of the tube wall decreases, a resistor that maintains a constant tube wall temperature will draw power. This power change indicates the degree of the decrease in tube pressure<sup>1</sup>. This gauge was electronically connected to the cold cathode using the controller (Pfeiffer TPG 300 with a CP300T11 measurement board) and thus the controller could switch back and forth and use the appropriate gauge at the appropriate pressure.

We heated the gauges to 80°C to keep molecules from condensing in them and clogging them. For this, we used band heaters (custom thin band heaters from Thermal devices that operated with a Watlow mini-J5R1-000 housed temperature controller and type J thermocouples) around the flanges that attached the cold cathode and pirani gauges (Figure 5.2 (6)) to the chamber. Because 80°C is below the decomposition temperature of all of the molecules used in the system, the presence of the heaters should have kept the molecules from condensing without having resulted in molecular decay.



---

We needed to measure the pressures of areas outside of the main chamber of the system. For one of these areas, we mounted a Pfeiffer (a TPR 018) pirani gauge to the stainless steel nipple (Figure 1.2 (7)) that connected the turbo pump to the gate valve of Dep 2. This pirani could measure pressures down to  $5 \times 10^{-4}$  mbar. In order to ensure that this nipple had enough ports to add this gauge and still have an extra port for an additional gauge if needed, we had Pascal add an additional port to the existing nipple. Other gauges were added between the turbo pump and the roughing pump (this area is known as the foreline) to verify that the roughing pump was functioning properly. A Pfeiffer angle valve was also added to this area (see Figure 1.2 (8)). A Televac thermocouple gauge was placed on either side of the angle valve (this gauge operates in a similar manner as a Pirani gauge) (9); thus, the pressure could be measured at either side of the valve. Additionally, a Granville-Phillips mini-convector gauge (10) (operates in a similar manner as a pirani) was placed between the turbo pump and angle valve so that the foreline pressure could be interlocked to the angle valve. Thus, if the roughing pump failed and the foreline pressure got too high, the angle valve would close and the backpressure of the turbo pump could be limited.

## Alkanethiol Source

Once the new pumping system was complete, we added two different molecular sources: one for liquid molecules and the second for solid molecules.

---

In order to vaporize molecules that were liquids at room temperature, we needed a way to simply leak the molecular vapor that collected above the liquid in a vial into the chamber. Thus, we attached a vial (Figure 1.3 (1)) to the vacuum chamber using a MDC precision leak valve (Figure 1.3 (2)). This quartz vial had a quartz-metal seal that connected the top open end of it to a conflat flange. This flange made it possible to connect the vial to a valve (a Varian right angle mini valve) (3) and maintain an ultra-high vacuum seal between the two. After the molecules were loaded into the vial and purified (see section 1.5), the valve (3) was attached to the vial and to the system.

Next, the scroll pump (Figure 1.3 (4)) was used to pump the air out of the area between the Dep 2 valve (Figure 1.3 (2)) and the vial valve (3). Once this area was at a pressure of approximately 100 mTorr, the valve to the pump was closed, and the valve to Dep 2 (Figure 1.3 (2)) was opened to bring the pressure of this area completely down to UHV. Then, the valve to system (2) was closed and the vial valve (3) was opened to allow the molecular vapor to fill the space between the vial and the system. Next, the system leak valve (2) was slowly opened to the desired setting so that the molecules were introduced to the system.

The ultimate molecular flux in the chamber depended on the leak valve setting, but also on the vapor pressure of the molecules. The higher the vapor pressure of the molecules used, the higher the chamber pressure could ultimately reach. Thus, if a flux of molecules was desired for an experiment that exceeded

---

the vapor pressure limits of the molecule used, the vapor pressure needed to be increased. This was accomplished for liquid sources by slightly heating them using a Brinkmann RM6 circulating bath (Figure 1.3 (5)) to raise the vapor pressure. The bath flowed water through a plastic hose to a copper coil that heated the water bath in which the vial was sitting (Figure 1.3 (6)). Thus, we were able to slowly heat the vial in a controlled manner and increase the molecular vapor pressure and the molecular flux.

However, simply heating the molecules in the vial did not adequately increase the molecular flux. This is because the heated molecules would then recondense on the cooler tubing in-between the source and the chamber. Thus, the area between the vial valve (3) and the system valve (2) was heated using two Watlow custom band heaters and heating tape. This area was heated to a temperature about 5 degrees higher than that of the circulating bath that heated the molecular source. This kept molecules from condensing on the tubing and increased the flux of the molecules at the sample with a dependence on the temperature of the circulating bath that heated the source.

- 1: vial with liquid source
- 2: MDC precision leak valve
- 3: Varian right angle mini valve
- 4: line to scroll pump
- 5: Brinkman RM6 circulating bath
- 6: water bath heated by copper coils with water from 5
- 7: quartz tube
- 8: bellows for liquid source
- 9: k-cell with bellows

- = existing equipment
- = liquid source added
- ▨ = low temperature k-cell added
- = ion gun added

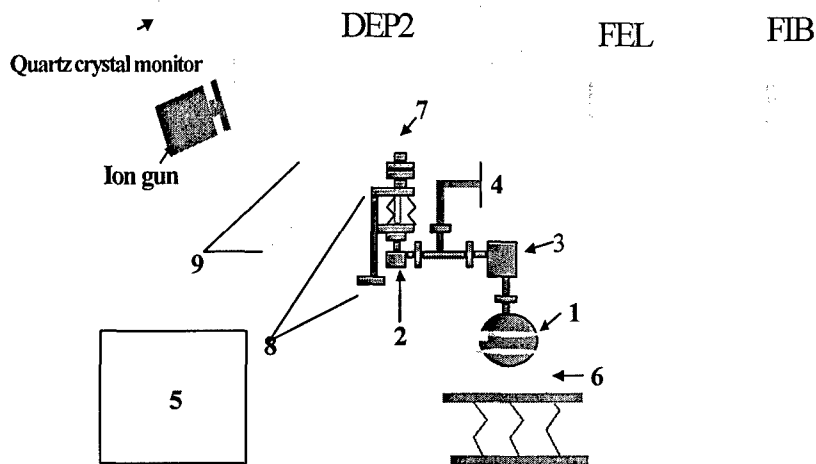


**Figure 1.3:** The back of Dep 2 showing the liquid and solid vaporization systems.

The leak valve (Figure 1.3 (2)) was connected to a flange on the system that held a quartz tube that extended up into the chamber (Figure 1.3 (7)). This tube was used to guide the molecules up through the system and to the sample. The flange with the tube was also connected to bellows (Figure 1.3 (8)). This allowed the tube to be extended or retracted in the system to change the distance

between the end of the tube and the sample and thus, change the flux of the molecules that reached the sample (since changing the flux using temperature was limited). When the bellows were fully contracted, the source to sample distance was approximately 1cm. However, this distance could be increased by up to 15cm. Below is a numbered photograph of the system with some of the same equipment as shown in Figure 1.3.

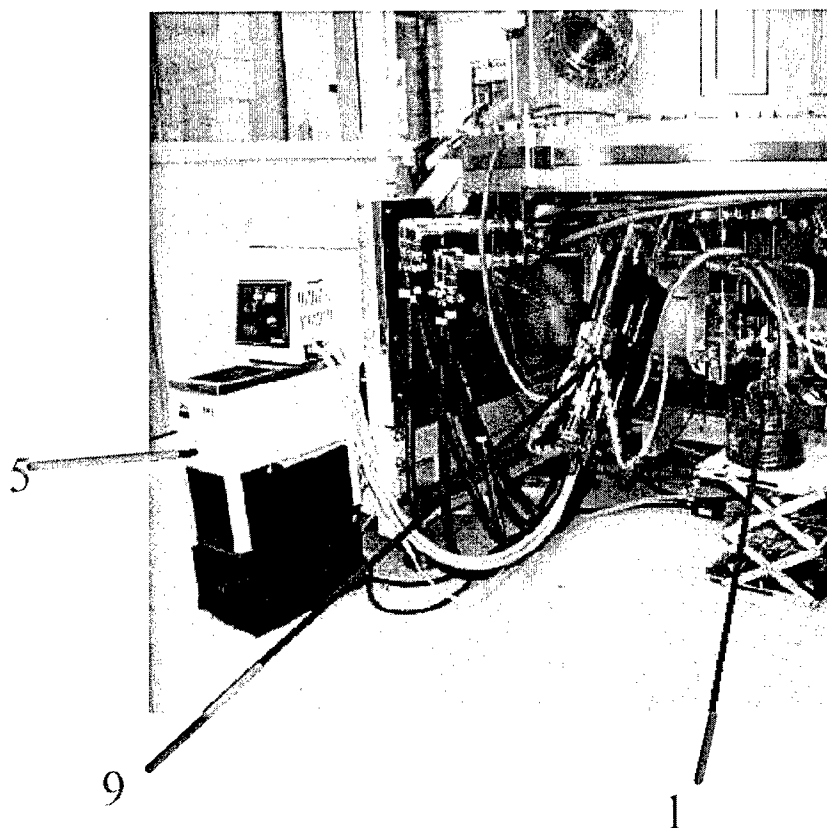


Figure 1.4: Photograph corresponding to diagram in Figure 1.3.

### Low Temperature Thermal Cell

The other molecules that we vaporized in Dep 2 (such as the OPE molecules) were in powder form at room temperature. Thus, they had to be heated to their vaporization temperature to reach a gaseous phase. However, there were several complications; one of which was that the sublimation and decomposition temperatures of these molecules were relatively low (only about

---

100-150°C). Thus, the molecules could not be vaporized using an electron beam. Further, standard sublimation cells do not operate controllably at these temperatures due to the fact that the power dissipation through radiation is strongly dependent on temperature (Stephen-Boltzmann's equation). Thus, for low temperatures, very little power can dissipate through radiation and the cell temperature cannot easily be controlled.

Another complication was that the decomposition temperatures for many of these molecules were sometimes only a few degrees higher than their sublimation temperatures. Thus, we needed a method to evaporate these molecules at relatively low temperatures and with excellent control; a 5-10 degree overshoot could cause the molecule to decompose.

Fortunately, we located a company that made thermal cells specifically for organic materials and that operated at low temperatures with excellent temperature control. This cell is shown in Figure 1.5. Its special features include a heating block that is heat-sinked by cooling water, thus, providing good temperature control at lower temperatures. Also, the contact between the material in the source and the heating is made using a liquid metal (Ga). This results in direct thermal contact between the heater and material ensuring that the filament does not have to overshoot in temperature to bring the source up to the desired temperature and thus, the source responds immediately to changes in the temperature of the heater. The placement of this cell on the chamber is shown in Figure 1.3 (9).

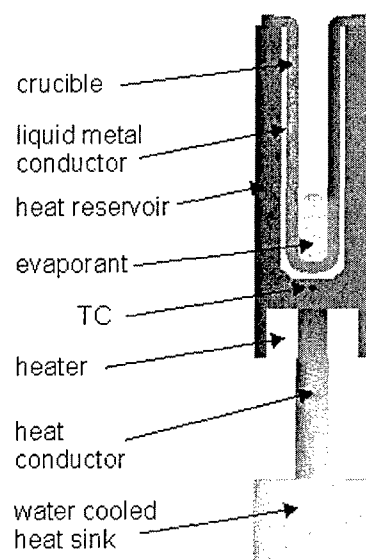


**Figure 1.5:** Diagram of the standard low temperature thermal cell used to vaporize powder molecules in UHV<sup>2</sup>.



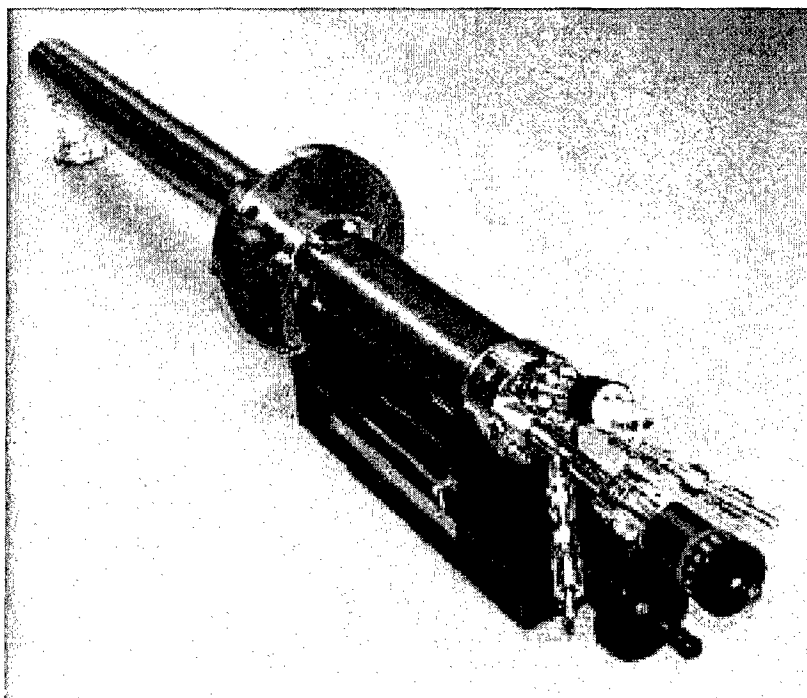


**Figure 1.6:** Photograph of our custom low-temperature thermal cell that includes an extended arm and bellows to control source to sample distance in-situ.

We added some features to our cell to meet our specific needs. We were not sure what ultimate source to sample distance we wanted for our molecules; additionally, we had little means to control the flux of molecules (since raising temperature was limited due to decomposition). Thus, we extended the cell arm and added a bellows system for changing the source to sample distance in-situ. The crucible with source material was placed in the end of the cell arm and

---

covered with a shutter. When the bellows were fully contracted, the source to sample distance was approximately 8 cm. However, the bellows could be retracted and the source to sample distance would then increase by up to 15 cm. In this manner, we were able to control the molecular flux during experiments in real time by changing the source to sample distance.

## **Liquid Molecule Purification Station**

Prior to vaporizing either of the sources, we first purified the molecules. Although the liquid molecules were purchased commercially and were rated over 95 percent pure, any impurities in nanoscale devices could affect the device results. Thus, purification of the liquid source was especially important. This purification consisted of a technique that is well known among chemists as freeze-pump-thaw cycles<sup>3,4,5</sup>. The apparatus used for these cycles is shown in Figure 1.8. Because alkanethiols are a pungent, possibly carcinogenic substance, they were loaded into the vial inside of a nitrogen glovebox. While inside of the glovebox, the vial was then capped with a closed leak valve.

In order to load the molecules into the vial in the glovebox, we had to build a stand that held the vial in an upright position so that the liquid alkanethiols did not spill out of the vial or into the leak valve. This stand also held the vial steady so that the bolts between the vial's conflat flange and that of the leak valve could be tightened in-situ (which required stability and dexterity considering the thick gloves of the glovebox).

---

Two different stands were built: one for a cylindrical vial and the other for a spherical vial. The stand for the cylindrical vial is shown below in Figure 1.6. This stand consisted of a heavy base (Figure 1.7 (1)) with four attached vertical rods and three platforms that were able to slide on these rods. One of these platforms held the flange that was attached to the top of the vial 1.7 (2), and a second held the flange of the valve 1.7 (3). The third platform held the heads of the bolts so that they stuck up through the bolt holes in the vial's flange 1.7 (4). Thus, in the glovebox, the liquid molecules were added to the vial, and then the platform holding the valve flange 1.7 (3) was lowered to sit flush with the vial flange 1.7 (2). Because the bolts had already been placed through the vial flange and were held there with a platform 1.7 (4), they went through the bolt holes in the valve flange when it was lowered flush with the vial flange. Then, the nuts were screwed onto the bolts that stuck up through the flanges and lastly, the platform holding the heads of the bolts in place 1.7 (4) was lowered and the bolts tightened completely. This apparatus made it easier to hold the vial in an upright position, to hold the bolts through both flanges, and to tighten them (all while the holder, vial, and valve were in a nitrogen environment).

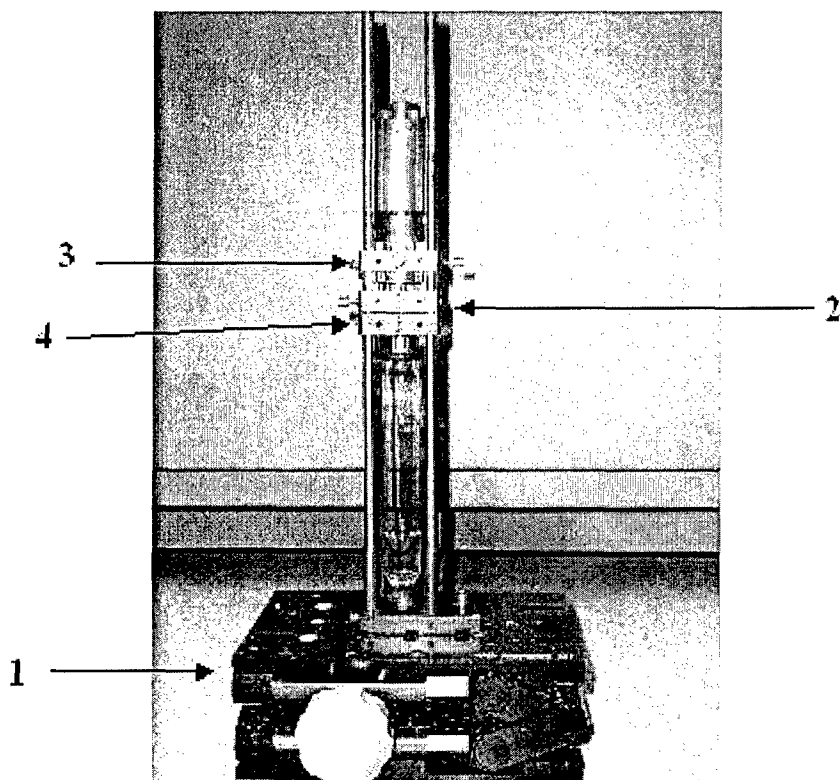


Figure 1.7: A photograph of the stand for loading the molecules into the cylindrical vial and attaching the leak valve in a nitrogen glovebox.

However, the holder shown in Figure 1.7 could not be used when we used a spherical molecule vial (the spherical vial was used to increase the surface area of the liquid molecules in experiments where we wanted a higher molecular flux in the chamber ) This was because the spherical vial did not fit on the base between the rods. Thus, a new, simple holder was built. For its base, a

---

spherical ball of Styrofoam that had a diameter greater than that of the vial had its center hollowed out to fit the vial snugly. The bottom of this ball was shaved off so that it would sit flatly on a bench. The vial could be placed in the stand and would be held in an upright position. Also, to hold the bolts in place through the vial's flange, prior to being loaded into the glovebox they were placed in position and taped with masking tape. After the vial was placed upright in the stand and was loaded into the glovebox, the liquid molecules were added and the valve was placed on top of the vial (aligned so that the bolts through the vial flange also stuck up through the valve flange). The top nuts were then screwed on finger tight, the masking tape holding the bolts was removed, the bolt heads were accessed, and the bolts were completely tightened. All of this was successfully done in the nitrogen glovebox.

Once the molecules were loaded into the vial using the appropriate stand in a nitrogen glovebox, freeze-pump-thaw cycles were performed to purify the molecules. First, the Varian mini angle valve (Figure 1.8 (1)) was attached to the top of the vial (Figure 1.8 (2)) and closed to seal the molecules in. The vial with the valve was then placed on the stand (Figure 1.8 (3)) and held by a clamp (4). A hose was used to connect the valve to a scroll pump (5). First, the pump was turned on and then the valve to the vial was opened so that the pump removed the gas from the vial. After the vial was at a pressure of less than 100 mTorr, the vial was closed. A container of liquid nitrogen (Figure 1.8 (6)) was raised up around the quartz vial using the jack (7) and the molecules were frozen. Once

---

frozen, the valve to the pump was opened to pump on the frozen molecules. Then, the valve was closed, and the bath of liquid nitrogen was replaced with a bath of tepid water and the molecules were thawed. As they thawed, bubbles escaped from the liquid as the contaminants with high vapor pressures left the liquid. Once the liquid stopped bubbling, the molecules in the vial were again frozen with liquid nitrogen, and the valve to the pump was opened to remove the gaseous contaminants from the vial. The valve to the pump was then closed and the molecules were thawed. These cycles were continued until after no bubbles were observed to escape from the liquid as it thawed-indicating that it had been purified. This generally took about five or six cycles. When finished, the thawed molecules were removed from the stand leaving the valve intact and closed. The vial valve 1.8 (1) was then attached to the system. Figure 1.9 shows a photograph of the freeze-pump thaw assembly with labels that correspond to those in Figure 1.8.

- 
1. Varian mini right angle valve
  2. Vial with solution
  3. Stand
  4. Clamp holding vial
  5. Line to Pressure gauge and scroll pump
  6. Container with liquid nitrogen or water
  7. Jack

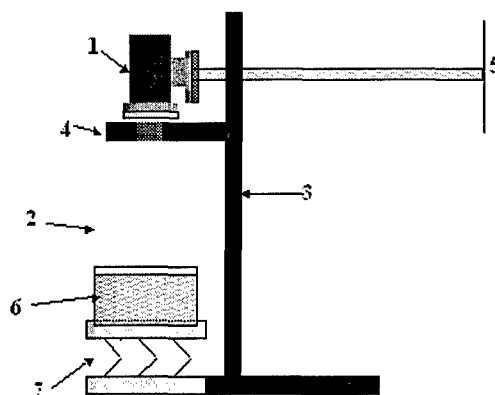


Figure 1.8: Purification system for liquid molecules.

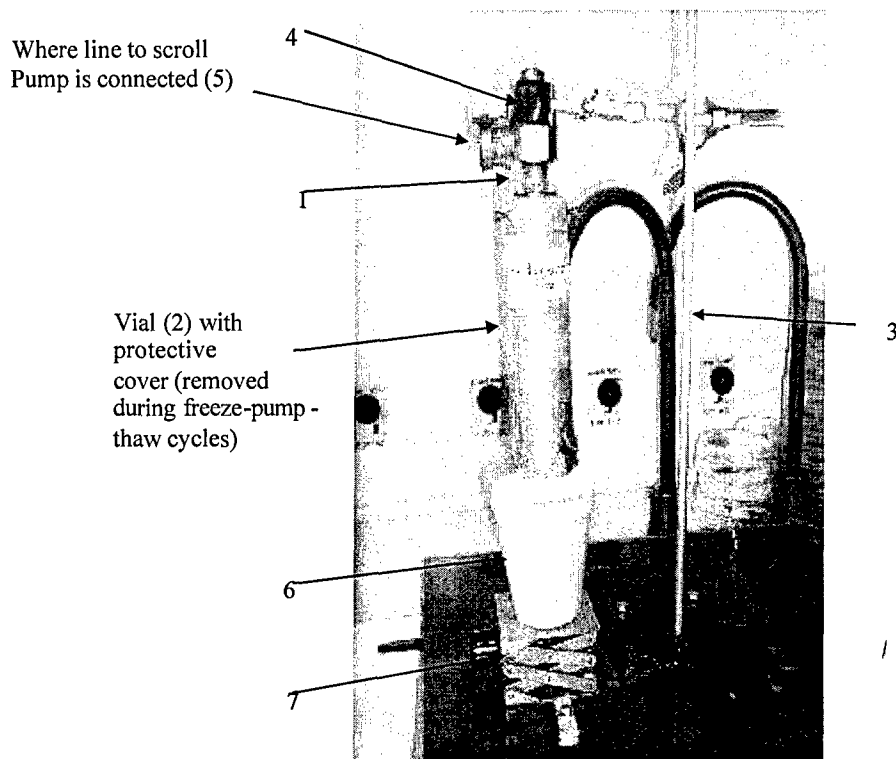


Figure 1.9: Photograph of the freeze-pump-thaw station, labeled corresponding to Figure 1.8.

## Powder Molecule Purification

The freeze thaw pump cycles would not have purified powder molecules, so we had to develop an alternative purification method. The design for this apparatus is shown in Figure 1.10. The purification station would remove materials with both higher and lower vaporization temperatures than the desired molecule. The molecules would be first loaded into what is to be the



---

heated area of the main quartz tube (Figure 1.10 (1)) inside of a nitrogen glovebox. A Thermionics straight through valve (Figure 1.10 (2)) would then be placed on the end of the quartz tube while it was still inside the glovebox and the valve would be closed before removing the tube from the glovebox to keep the molecules from being exposed to the environment. The valve would be attached to the tube using an adaptor that has an o-ring tube coupling on one end and a quick flange (kf) on the other 1.10 (3). This valve and tube would then be loaded into the light proof assembly that holds the system 1.10 (4) and the kf flange of the valve would be connected to the kf flange that connects to a line to the turbo pump 1.10 (5). The Pfeiffer TSU 071E Economy Pumping Station turbo pump 1.10 (6) would then be turned on, the valve to the tube opened, and then the nitrogen from the glovebox pumped out of the tube.

To purify the molecules, the temperature of the Linn High Therm mini tube furnace would be slowly raised to the sublimation temperature of the molecules. When the temperature inside the heated area of the tube is lower than the sublimation temperature of the molecules, the molecules would not sublime, but contaminants with lower sublimation temperatures would. These contaminants would either remain in the gas phase and be removed by the turbo pump, or would condense when they arrive in the cooler area of the tube. A separate sleeve would be placed inside of the tube in the cooler forward area of the tube to collect these higher vapor pressure contaminants (See Figure 1.10 insert (1)). In order to prevent these contaminants from

---

clogging the turbo pump, a micromaze filter was placed in the line between the tube and the pump (Figure 1.10 (7)). Additionally, the turbo pump has a purge valve so that nitrogen can be purged over the bearings to prevent further clogging with molecules. The pressure of the line will be measured by a Pfeiffer PKR 251 compact pirani/cold cathode gauge (Figure 1.10 (8)).

Once the heated area (Figure 1.10 insert 1) reaches the sublimation temperature for the molecules, the heated area would be kept at this exact temperature and the molecules will sublime. However, they should condense as soon as they reach a slightly cooler area of the quartz tube (condensed target material area in insert 1). For this reason we would place another sleeve in the area of the tube where the temperature drops slightly below that of the sublimation temperature. Thus, the desired molecules should condense and collect here. The leftover product in the heated area of the sleeve would be lower vapor pressure contamination and thus it too would have its own sleeve. When the molecular sublimation is complete, the turbo pump would be turned off, the tube with the valve intact removed, and the valve opened and removed once the tube is in the nitrogen glovebox. The sleeve with the desired condense material would be removed, and the molecular material loaded into an airtight vial. This material could then be loaded into the thermal cell for vaporization. Although this station was designed and built, it has not yet been used. Currently, the molecules are purified in the chamber by heating the source to a temperature immediately

below the vaporization temperature of the molecules. This is done before any samples were loaded into the chamber, thus the contaminants vaporize, enter the chamber, and are pulled away by the turbo pump. Figure 1.10 shows a photograph of the equipment in Figure 1.11

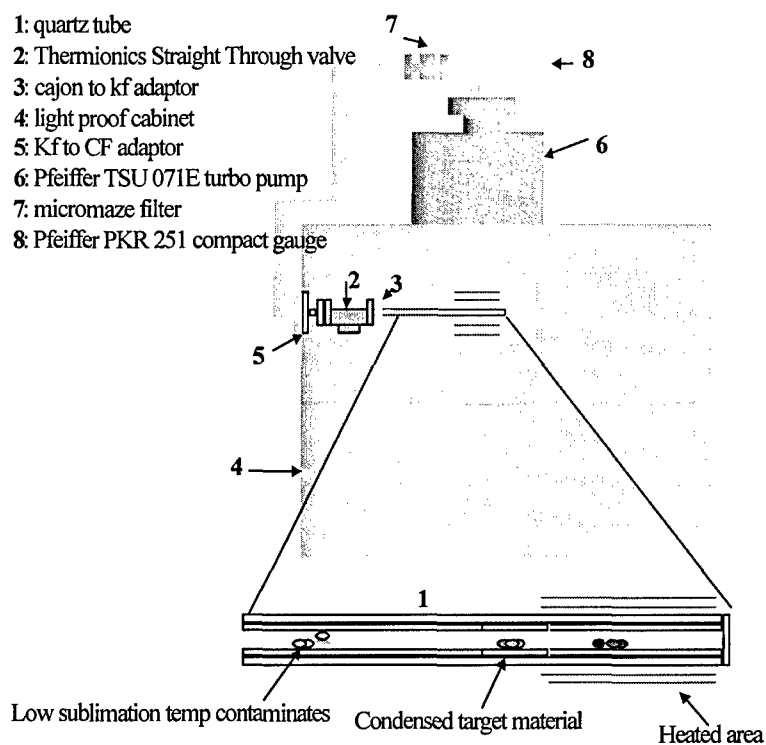
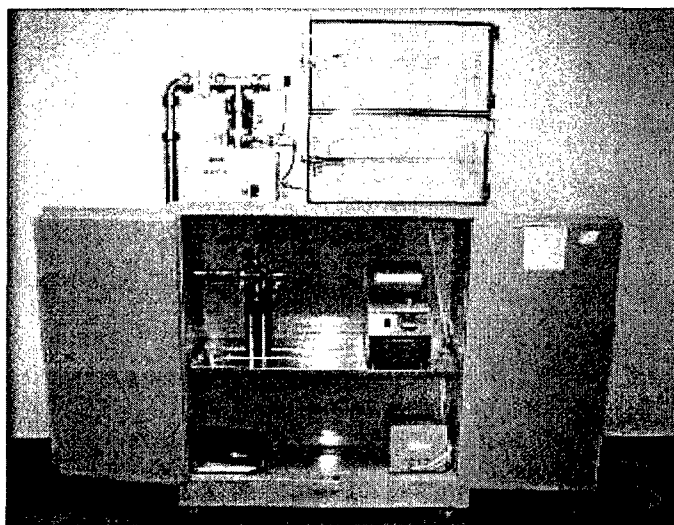


Figure 1.10: Powder molecule purification station.



**Figure 1.11:** Photograph of the powder molecule purification station.

---

### Works Cited for This Section

1. William F Brunner, *Practical Vacuum System Techniques*, an unpublished manual for Bell Labs, 1983.
2. Image from MBE Komponenten, [www.mbe-components.com/products/effusion/ome.html](http://www.mbe-components.com/products/effusion/ome.html).
3. G.E. Poirer et al, *Langmuir* **15**, 1167 (1999).
4. H. Kondoh et al., *Journal of Chemical Physics* **111** (3), 1175 (1999).

- 
5. Lonergan Group, an unpublished process sheet, Department of Chemistry, Materials Science Institute, University of Oregon, [www.uoregon.edu/~lnrgn/Assets/FPT.pdf](http://www.uoregon.edu/~lnrgn/Assets/FPT.pdf).

## Vapor Phase Results: Alkanethiols

Once the vapor phase deposition system was designed and constructed, we used it to assemble various monolayers of organic molecules. The first molecules that we assembled were alkanethiols. This was because there existed literature precedents for the vapor phase deposition of monolayers of alkanethiols in an ultra-high vacuum environment<sup>1-5</sup>. This previous work showed that when alkanethiol molecules were vaporized on a gold substrate using an adequate exposure, dense monolayers were formed with the molecules in the "standing up phase"<sup>1-5</sup>. This final dense monolayer is desired for use in molecular electronic devices.

The following sections describe the work that we performed for achieving vapor phase deposition of alkanethiol molecules. This work included vaporizing both C6 (alkanethiols 6 carbons long) and C12 (alkanethiols 12 carbons long) on gold. STM images of the C12 monolayers confirmed that we achieved an adequate flux for forming the desired dense standing up structure<sup>13</sup>. We then used vapor phase deposition to assemble a monolayer of the C12 molecules in the nanowell device and tested the device electrically at room temperature to confirm that the monolayer exhibited the expected electrical characteristics.

## Experimental Procedure for Vaporizing Alkanethiols

Prior to the vaporization of alkanethiols, the molecules (purchased from Sigma Aldrich and 98% pure) were purified. This purification was performed using the apparatus for freeze-pump-thaw cycles<sup>6</sup>. After purification, the valved off vial of molecules was loaded onto Dep 2.

Prior to performing experiments with new molecules, we had to establish how the chamber pressure changed as the leak valve to the molecules was opened to various settings. By establishing this, we could predetermine what leak valve setting was needed to achieve the chamber pressure required for a specific sample exposure (this chamber pressure/substrate exposure relationship is described in greater detail in section 2.2). This was done by first slowly opening the leak valve and watching the chamber pressure. When the chamber pressure reached and held the desired value, the leak valve setting for this pressure was recorded.

After the valve calibration, the gold substrates were loaded face down into tantalum rings and into the fast entry load lock (FEL) of the dual system chamber. These substrates consisted of 5nm of titanium followed by 200nm of gold evaporated on p-type silicon (100) wafers. The metals were evaporated in an electron beam evaporator at rates of 1 Angstrom per second and 10 Angstroms per second respectively. The wafers that were to be imaged with scanning tunneling microscopy (STM) after molecular assembly were flame annealed



using a hydrogen-oxygen flame. This flame annealing was performed to increase the grain size of the gold to improve the STM image quality. Wafers that were flame annealed were not chemically cleaned prior to being loaded into the chamber (since the flame annealing should have helped to remove wafer contamination). The wafers that were not flame annealed were cleaned prior to being loaded into the chamber using a standard piranha clean (sulfuric acid: hydrogen peroxide 3:1).

At least an hour prior to the vaporization of the molecules the heaters and the water bath were turned on to heat up and reach equilibrium temperatures. These heaters included: the two band heaters on the gauges (80 °C), and the two band heaters and heating tape on the area between the vial shut-off valve and the Dep 2 leak valve. The water bath was also turned on and set to 55° C. The water bath was not used for the C6 molecules because they had a vapor pressure high enough at room temperature to result in an adequate flux at the substrate. However, the C12 molecules had a vapor pressure that was too low at room temperature, so we heated the C12 molecules to 55 °C for each run.

After the water baths and all heaters had reached equilibrium, the turbo pump was switched to full speed mode and the wafers were loaded from the FEL to Dep 2. Then, the quartz tube that guided the molecules from the vial to the sample was moved up using the bellows to approximately 1 cm from the sample (bellows indicator at 125mm). The leak valve on Dep 2 was then opened to the determined setting for the desired chamber/substrate pressure and left

open for the desired time. After the time required for the experiment, the vial was closed and the wafer left in the chamber until the chamber pressure dropped back to approximately the base pressure (typically around  $2 \times 10^{-8}$  mbar). The wafer was then removed from the FEL and scribed into pieces approximately 1cm x1cm. These pieces were then imaged with the STM to check for ordering that indicated a dense monolayer

After the experimental runs, the water bath was turned off immediately, but the band heaters were left on for another 2 hours after the vaporization to allow the molecules to condense in the vial. After these heaters are turned off, the vial was covered in aluminum foil to minimize exposure to light.

### **Estimation of Sample Pressure/Chamber Pressure for Alkanethiols**

As mentioned in the previous section, in order to calculate exposure (which is required to ensure a dense standing up monolayer<sup>1,3</sup>), the pressure at the sample must be known. However, the pressure gauge closest to the sample is the cold cathode, which is located in the upper area of the chamber, approximately 30cm away from the sample. The sample pressure should change proportionally to the molecular chamber pressure (indicated by the cold cathode gauge), so the chamber pressure can be used to estimate the sample pressure. Additionally, assuming that the molecules disperse into a hemisphere from the opening of the quartz tube (taken to be a point source) and that the molecules are

then removed from the system, one can estimate the pressure relationship between the gauge and the sample. Since the source to sample distance is estimated to be 1cm and the source to gauge distance is estimated to be 30cm, the relationship would be:

$$\text{Surface\_area\_hemisphere\_source\_sample} = \frac{1}{2} (4 \pi r^2) = 6\text{cm}^2$$

$$\text{Surface\_area\_hemisphere\_source\_gauge} = \frac{1}{2} (4 \pi r^2) = 5,600\text{cm}^2$$

$$(\text{source to gauge area})/(\text{source to sample area}) = 5,600\text{cm}^2 / 6\text{cm}^2 = 930:1$$

This estimation shows that the sample should see about 1,000 times the pressure as the gauge sees. For example, the required exposure of C6 for a dense monolayer of C6 is approximately 50,000L<sup>1</sup> (1 Langmuir (L) =  $1 \times 10^{-6}$  Torr x sec). A Langmuir is a unit of exposure that is commonly used by surface scientists. One Langmuir of exposure is approximately equal to one monolayer of exposure. When the chamber pressure gauge reads a pressure of  $1 \times 10^{-7}$  mbar, or  $7.5 \times 10^{-8}$  Torr, the estimated sample pressure would be  $7.5 \times 10^{-5}$  Torr. So, for 50,000 L of exposure at the sample surface, a chamber pressure of about  $1 \times 10^{-7}$  mbar would have to be maintained for about 660 seconds or 11 minutes.

Alternatively, we could have estimated the sample pressure based on the molecular flow from the vial into the chamber. This could have been

determined using the fact that the flow would equal the pressure difference between the vapor pressure of the molecules in the vial and the pressure of the chamber, divided by the total resistance to the flow between the vial and the chamber<sup>7,8</sup>. However, for this, the resistance of the Dep 2 leak valve would need to be known. Since we did not have this information, we relied on the sample pressure estimations based on the chamber pressure.

## STM Results for the Alkanethiol Monolayers

The first experiments performed were with C6 molecules. The literature showed that the dense standing up monolayers of these molecules were formed by exposing the gold substrates to approximately 50,000 L of molecules<sup>1-4</sup>. We thus, followed the estimation method described in section 6.2 to achieve an exposure greater than that in the literature by exposing our wafers to C6 at a chamber pressure of  $3 \times 10^{-6}$  mbar for 30 min.

We used scanning tunneling microscopy (STM) to characterize the monolayers after assembly. If the STM showed "striping", we could confirm that a single chemisorbed monolayer had been formed. Although we followed the literature precedent for forming an ordered monolayer of C6 via vapor phase, we were unable to observe any ordering when we imaged the monolayers with STM (see Figure 2.1). We were not sure if this was due to the molecules not forming ordered monolayers on the surface, or due to imaging problems that resulted from the short chain length of the molecules (if the molecules are too

short to provide enough contrast with the underlying gold this striping may not be observed). It is well established that C6 forms ordered monolayers when assembled from the solution phase. However, we were unable to observe any ordering in the C6 molecules even when they were assembled from solution phase (shown below in Figure 2.2). This may be due to the imaging capabilities of the STM (which unlike those used in the literature was not a state-of-the-art UHV STM<sup>1-4</sup>). Thus, we attributed the lack of order observed not to the vapor phase deposition procedure, but the STM characterization limitations.

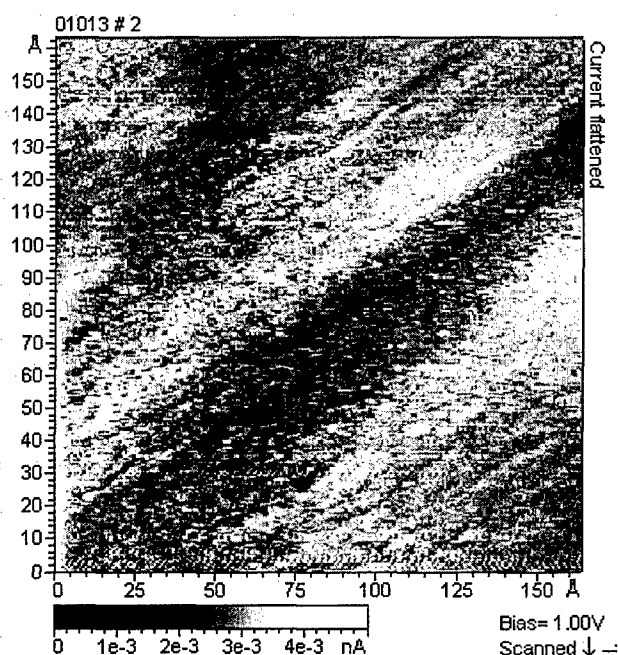


Figure 2.1: STM image of C6 on gold assembled via vapor phase deposition, imaged using a Pt/Ir tip and 1V, 10 pA, no "striping" evident.

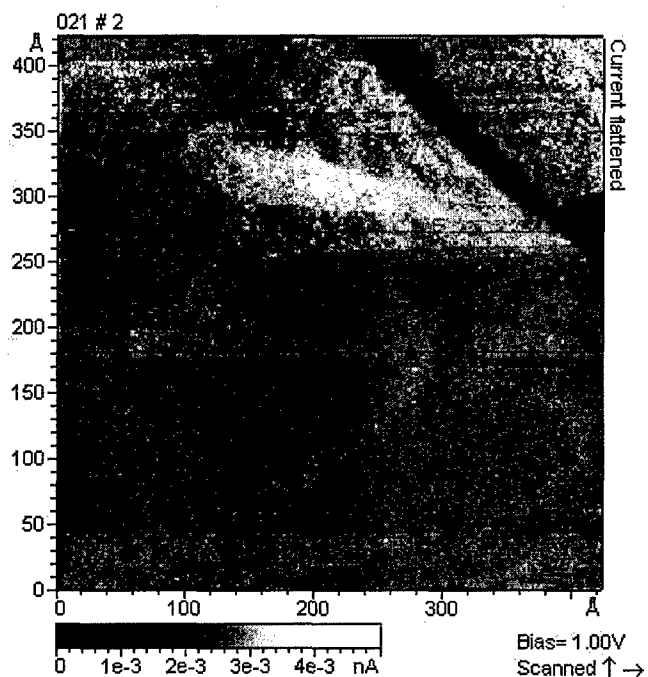


Figure 2.2: STM image of C6 on gold assembled via solution phase deposition, imaged using a Pt/Ir tip and 1V, 10 pA, no "striping" evident.

Because we had successfully observed order from the STM images of C12 when assembled from solution phase, we decided next to attempt to vaporize C12 molecules. However, in our first attempts, we realized that the maximum chamber pressure that we could achieve by opening the leak valve to the molecular source at room temperature was inadequate for achieving the desired substrate exposure of molecules. This may explain why we were unable to find any reports of successful dense well-ordered monolayers of C12 being assembled from the vapor phase. This low chamber pressure was due to the relatively low vapor pressure of the longer molecules.

After the first attempts to increase the vapor pressure by heating the C12 molecules using the circulating bath, we were still not achieving the desired pressure in the deposition chamber. We thus moved from storing the molecular source in a cylindrical vial to storing the molecules in a spherical vial to increase the vaporization surface area. Although this increased the chamber pressure a miniscule amount, we eventually discovered that the limiting factor in the chamber pressure was not the heating nor the surface area of the molecules, but rather that the molecules were condensing in tubing between the vial and the chamber. This was because although the molecular source was heated, we did

not heat the tubing and leak valve leading from the source into the chamber. Once this area was heated, the molecules no longer condensed in the tubing and we only had to heat the molecular source to approximately 55° C in order to achieve the desired chamber pressures.

The first experiments we performed for assembling C12 on gold were performed using a chamber pressure of  $3 \times 10^{-6}$  mbar for 30 minutes. When these monolayers were characterized using STM, no order was observed even though the exposure was similar to that other groups had used in the literature for the formation of vapor phase assembled monolayers of C6<sup>1</sup>. We wondered if perhaps the growth rate was too fast and thus not allowing the molecules enough time to move around on the surface and order. Thus, we next attempted to vaporize C12 molecules on gold using a chamber pressure of  $5 \times 10^{-7}$  mbar for 200 minutes (the same total exposure as  $3 \times 10^{-6}$  mbar for 30 minutes). When imaging these monolayers with STM, we were able to observe ordering that was consistent with that reported in the literature for the dense standing up phase of alkanethiols assembled on gold<sup>1-5</sup>. An STM image of C12 that was assembled on flame-annealed gold using these conditions is shown in Figure 2.3.



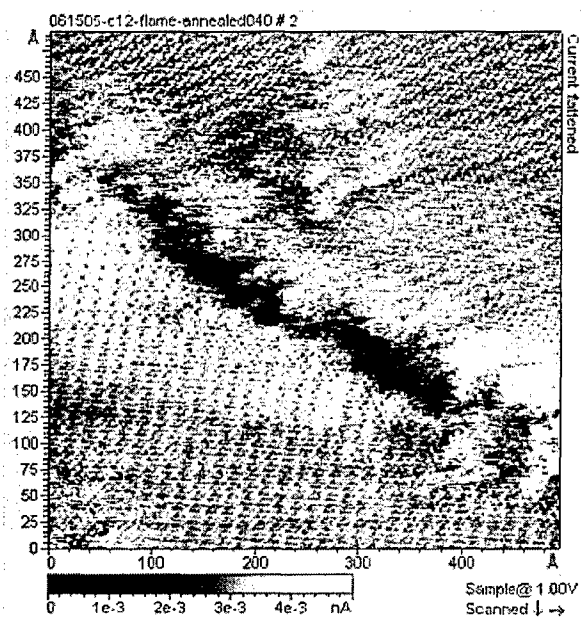
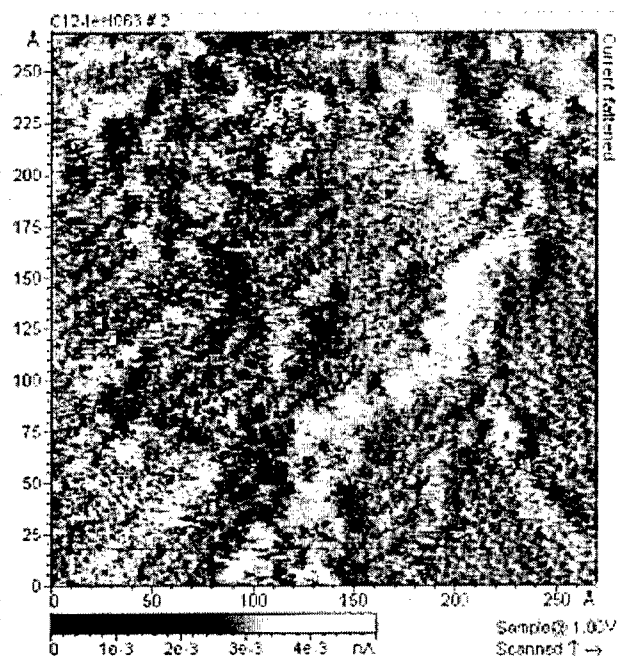


Figure 2.3: STM image of C12 on flame-annealed Au assembled via vapor phase deposition, imaged using a Pt/Ir tip and 1V, 10 pA, ordering evident.



**Figure 2.4:** STM of C12 on Au assembled via solution phase deposition imaged using a Pt/Ir tip and 1V, 10 pA.

The ordering observed from the STM image of vapor phase deposited molecules on Au was similar to that observed from the C12 monolayer assembled from solution phase deposition. The pitch between the “stripes” observed for each of these monolayers was measured to range from about 9-13 Angstroms. This pitch matches that shown in the literature expected for the

most dense phase of alkanethiols assembled on gold<sup>13</sup>. This range was observed between different samples as well as in different areas of the same sample. It could be due to artifacts due to the tip imaging monolayers on different heights of gold grains, or perhaps the monolayer exists in slightly less dense phases in parts of the monolayer. However, the same range of pitch values were observed for the vapor phase as the solution phase assembled monolayers.

### **Alkanethiol Nanowell Devices Fabricated via Vapor Phase Deposition**

After establishing that vapor phase deposition could be used to assemble molecules on gold wafers and achieve a dense ordered layer, we used the established conditions (given in section 2.3) to deposit alkanethiol molecules in nanowell devices. First, 100nm wells were milled using focused ion beam (FIB). Then, the chips were cleaned with piranha (sulfuric acid and hydrogen peroxide in a ratio of 3:1) and loaded into the tantalum chip holder and into the FEL. This chip holder had holes to expose the center of each chip where the nanowells were milled. Then, the established procedure for assembling C12 molecules via vapor phase was followed (turn on heaters and bath, load in sample, raise tube so that it is 1cm from the sample, open valve until chamber pressure is  $5 \times 10^{-7}$  mbar, and run for 200 minutes). After the chips were removed, they were immediately loaded into the shadow mask used for evaporating the top gold contacts on the nanowells and into the electron beam evaporator. The

evaporator was pumped down to a pressure of approximately  $1 \times 10^{-7}$  Torr, and Ti and Au were evaporated at rates of 1 and 10 Angstroms/sec respectively.

After removal from the evaporator the chips were probed at room temperature using the HP 4145B. The IV characteristics from the nanowell devices with molecules assembled from vapor phase were similar to those from C12 molecules assembled from solution phase. The room temperature IV characteristics are shown below in Figure 2.5 and the I-V characteristics for C12 assembled via solution phase are shown in Figure 2.6. As one can see from these curves, the I-V characteristics of the vapor phase assembled monolayer are qualitatively similar to those from monolayers assembled via solution phase.

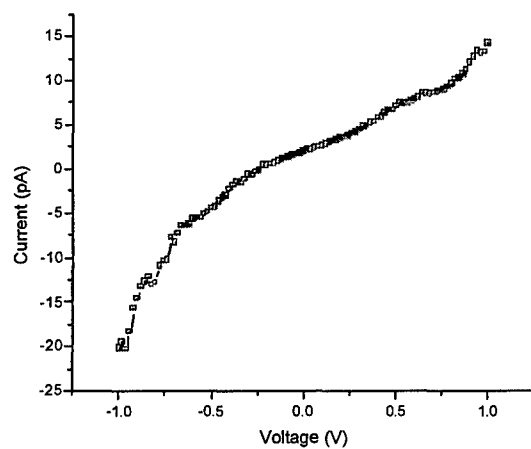


**Figure 2.5:** The I-V characteristics for a C12 monolayer assembled via vapor phase deposition in a nanowell device.

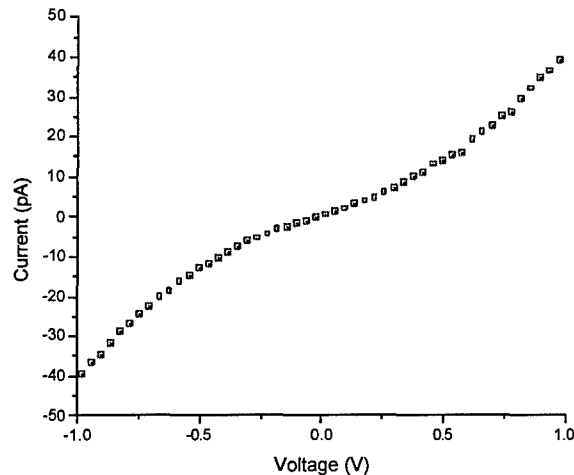


**Figure 2.6:** The I-V characteristics for a monolayer of C12 molecules assembled via solution phase deposition in a nanowell device.

Comparing the I-V curves in Figures 2.5 and 2.6, the curve from the vapor-assembled monolayer shown in Figure 2.5 is slightly more linear than that of Figure 2.6. This linearity was observed when the curve was fit to the Simmons equation. The vapor assembled IV characteristics fit the Simmons equation with  $\phi$  value approximately 10% higher than that found for alkanethiol molecules assembled in the nanowell device from solution phase. This  $\phi$  value indicates that the vapor phase deposited monolayer had a slightly larger potential barrier than those deposited from solution phase. This barrier could

have resulted from the alkanethiol films in the nanowell being thicker than a monolayer.

If the films were thicker than a monolayer in some areas, this may not have been detected by STM. This is because the imaging technique of STM identifies order only over an area less than  $100 \times 100$  nm, not the entire sample. Additionally, experience has shown that the STM current may actually penetrate through a disordered top layer of molecules and image a densely packed bottom monolayer of molecules. Thus, we are confident that we were able to deposit an ordered chemisorbed monolayer of alkanethiol molecules on gold, but are not positive that there were not additional physisorbed molecules on top of the monolayer. It is important to note that monolayers deposited via solution phase deposition also have physisorbed top molecules and are thus rinsed with solvents to get rid of them.

The nanowell devices fabricated via vapor phase assembly showed higher yields than those deposited via solution phase. Our yields of devices that were not electrically open or short when probed went from about 6% for C12 monolayers assembled via solution phase to 28% for devices assembled via vapor phase. These yields are based on testing more than 100 of each of the two types of devices. However, we later noticed for other molecules that device yield seemed to correlate with monolayer thickness (the idea being that films thicker than a monolayer have less of a chance of the top metal penetrating through them). Thus, we are unable to conclusively attribute our increased

yield to the vapor phase deposition process, rather than the thickness of the monolayer that may have resulted from vapor phase deposition.

We were able to use the newly assembled vapor phase deposition system with the source of the liquid molecules to assemble a monolayer of alkanethiols on gold. The ordering of this monolayer was confirmed using STM and was shown to be similar to that observed from solution phase assembled monolayers. The molecules used were longer than those previously reported assembled via vapor phase in an ultra-high vacuum environment and thus, had to be heated slightly in order to achieve the flux necessary. We also assembled an ordered monolayer of C12 via vapor phase deposition in a nanowell test device. This device showed electrical results that were qualitatively similar to those observed from a nanowell device fabricated via solution phase assembly. These IV characteristics indicated that the vapor-phase deposited film might not have consisted of exactly a monolayer of molecules. Overall, we established a method to deposit approximately a monolayer of ordered C12 on gold via vapor phase. The following section describes how we attempted to establish the conditions for assembling a single ordered monolayer of conjugated molecules on gold.

## **Works Cited for This Section**



1. H. Kondoh et al, *Journal of Chemical Physics* **11** (3), 1175 (1999).
2. F. Schreiber et al, *Physical Review B* **57** (19), 57 (1998).
3. G.E. Poirier et al, *Langmuir* **15**, 1167 (1999).
4. F. Shreiber, *Progress in Surface Science* **65**, 151 (2000).
5. J.C. Love, *Chem. Rev.* **105**, 1103 (2005).
6. Lonergan Group, unpublished process sheet, Department of Chemistry,  
Materials Science Institute, University of Oregon,  
[www.uoregon.edu/~lnrgn/Assets/FPT.pdf](http://www.uoregon.edu/~lnrgn/Assets/FPT.pdf).
7. A. Guthrie, R.K. Wakering, *Vacuum Equipment and Techniques*, McGraw-Hill Book Company Inc, New York, 1949.
8. A. Chambers et al., *Basic Vacuum Technology*, IOP Publishing Ltd, New York, 1989.

## Vapor Phase Results: OPEs

After verifying that we were able to use vapor phase deposition to assemble dense ordered monolayers of alkanethiols on Au, we moved on to assemble monolayers of oligo (phenylene ethynylene) OPE molecules on Au. These molecules are of interest because they are much better conductors than alkanethiols. Also, they are the base for the more interesting molecules that have been observed to show switching behaviors<sup>1-19</sup>. If one is able to successfully assemble these "plain" OPE monolayers using vapor phase deposition, it is likely that similar procedures could be used to vaporize and assemble variations of the OPEs molecules (various sidegroups etc). However, it should be noted that unlike the alkane work, there were no prior reports of ordered OPE monolayer assembly via vapor phase deposition (actually, it had been reported that ordered vapor phase assemble would not occur<sup>20</sup>).

If vapor phase deposition of OPEs could be achieved, it could improve the quality and reproducibility of monolayer assembly, thus leading to improved device yields and reproducibility of device results. The existing standard of monolayer assembly, solution phase, starts with molecules that are often only 98% pure and uses solvents that can further contaminate the monolayer. To address these issues, some groups have attempted "gas-phase" deposition of OPEs (the substrate is placed in a closed vessel of nitrogen and the molecules are heated in the same vessel to produce a gas, which assembles on this substrate<sup>20-</sup>

22). However, this method has similar contamination and consistency issues as seen in solution phase deposition and often produces multilayers, rather than a monolayer<sup>20</sup>.

We built on the knowledge gained from vapor phase assembly of alkanethiol molecules and used the modified low temperature thermal cell for the vaporization of the OPE molecules in an ultra-high vacuum (UHV) chamber. The following sections describe how we used this cell to strictly control the temperature of the molecular source to achieve the desired molecular flux without causing molecular decay. We confirmed that the monolayers we assembled were single uncontaminated, chemisorbed, and ordered using the characterization techniques of ellipsometry, x-ray photoelectron spectroscopy (XPS), and scanning tunneling microscopy (STM). We then used vapor phase deposition to assemble the molecules in a nanowell test device.

### **Experimental Procedure for Vaporizing OPEs**

The molecules that were used for this work were simple OPE molecules with a thiol endgroup (see Figure 3.1). We started with OPEs because they are the backbone of molecules currently assembled on gold for use in molecular test devices<sup>1-19</sup>. The OPEs were synthesized at Rice University using standard protocols<sup>23</sup>. The substrates used for this work were silicon wafers with 5nm of evaporated titanium covered with 200nm of evaporated gold. We used these gold-coated substrates because of the established thiol-Au bonding mechanism.

For solution phase assembly of OPEs it is common to use molecules with the sulfur endgroups that are "protected" with an acetyl group to help reduce the chance of molecular oxidation and degradation prior to use. However, since we did not want to expose the molecules to solutions prior to assembly to remove this endgroup (to reduce chances of contamination), we used "unprotected" molecules (Figure 3.1). We thus had to make sure that the molecules had extremely limited exposure to light and air. Prior to use, the molecules were kept in a freezer in a closed container of nitrogen only exposed to air and light for the few minutes required to load them into the thermal cell UHV chamber. All of the view ports of the UHV chamber were covered to keep out light. Approximately 10-20mg of molecules were loaded into the quartz crucible in the thermal cell at a time.

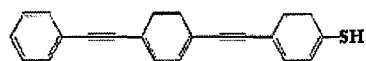


**Figure 3.1:** An OPE molecule.

In order to assemble a monolayer of the OPE molecules we had to establish the source temperature that would be needed for vaporization. Thermal gravitational analysis (TGA) of the OPE molecules showed that there was very little molecular vaporization at source temperatures up to 350°C.

However, if all vaporizing molecules reached the substrate and condensed to form a monolayer (which we believed the OPEs did), the weight of molecules used would be less than 1 microgram, which the TGA was not sensitive enough to measure. Thus, we were not able to rely on the TGA results for the vaporization temperature of the OPEs. We thus performed our first experimental run at a source temperature of 150°C for 200 minutes (these starting conditions were estimated based on what was required to form an alkanethiol monolayer). We kept the source temperature below 152°C because that is the temperature that was identified via differential scanning calorimetry as the molecular decomposition temperature. These run conditions resulted in a film that was determined via ellipsometry to be more than 100 monolayers thick. We then reduced the source temperature and exposure time until we could assemble a film in less than one hour that was approximately one monolayer thick (120°C-130°C). We were then able to refine our temperature/exposure times for achieving exactly one monolayer of molecules (described below).

Prior to deposition, the molecules were purified in-situ. This procedure was performed with no substrate in the deposition chamber and the source shutter open. First, the temperature of the thermal cell was slowly increased to just above the molecular vaporization temperature (around 130°C). Typically during this degassing, the deposition chamber pressure would increase from  $2 \times 10^{-8}$  mbar to  $8 \times 10^{-7}$  mbar (we interpret this increase in pressure to the vaporization of any molecular source contamination). We then held this

temperature until the deposition chamber pressure returned to the  $2 \times 10^{-8}$  mbar range, indicating that all of the volatile contaminants were out of the source and it was purified. After the in-situ purification, we observed no increase in pressure when the molecules were later vaporized (even when growing films that were 10 or more monolayers thick). This indicated that the OPE molecules condensed immediately on the first surface without reaching the gauges.

Prior to assembling the OPEs, the gold-coated substrates were first cleaned with a piranha etch (sulfuric acid and hydrogen peroxide in a ratio of 3:1). The substrates were then immediately loaded into the UHV chamber. Before the wafer was moved into the deposition chamber, the temperature of the thermal cell was ramped up to 80°C. The wafer was then loaded into the deposition chamber with the gold side facing the source. The molecular source was then raised (using a bellows system on the thermal cell) to a distance approximately 8cm from the center of the sample, the source shutter was opened, and the cell temperature increased to the vaporization temperature. The cell temperature overshoot, as indicated by an integrated thermocouple, was less than 0.4°C. After the deposition was complete, the temperature of the cell was slowly ramped down, and the substrate was removed from the deposition chamber for characterization.

For this work, we first performed experiments that varied the flux of molecules to the substrate by changing either the time or the temperature of the exposure. After deposition, several characterization techniques were performed

to establish how the film thickness varied with exposure, as well as to establish the conditions required for assembling a chemisorbed, dense, ordered monolayer. These characterization techniques included scanning tunneling microscopy (STM) (performed at the University of Virginia), ellipsometry (performed at Rice University), and x-ray photoelectron spectroscopy (XPS) (also performed at Rice University).

### **Ellipsometry Results for the OPE Monolayers on Gold**

Ellipsometry was performed at Rice University and was used to verify that the vapor deposited films were dense monolayers. The graphs in Figure 3.2 show the film thickness as determined by ellipsometry for various molecular exposures. Figure 3.2 (a) shows thickness versus source temperature for samples with a constant exposure time of 30 minutes, and Figure 3.2 (b) shows thickness versus time for samples with a constant source temperature of 130°C. Each graph shows data from the very center of the 2-inch wafers, as well as from the edge of the wafer farthest from the source. The center samples were approximately 8cm from the source, whereas the edge piece was approximately 9.5cm from the source. Each point on each graph shows the average sample thickness of 1cm x 1cm area. Different measurements taken at slightly different areas of the same 1 cm x 1 cm samples showed average thickness variations of 8%.

The ellipsometry showed that a variety of conditions could be used to assemble a film with a thickness of approximately 23 Angstroms (the thickness theorized for 1 monolayer of OPE on Au<sup>24</sup>). Figure 3.2 shows the film thickness for a constant source temperature and various exposure times (a), and for various source temperatures with a constant exposure time (b). As one can see in Figure 3.2 (a), a film that was one monolayer thick was observed from the center of the wafer when it was exposed to OPE molecules that were heated to temperatures between about 121 and 123°C for 30 minutes. This monolayer thick film was observed at the edge of the wafer when it was exposed to molecules that were heated at 125 °C for 30 minutes. As Figure 3.2 (b) shows, the film was one monolayer thick in the center of the wafer after the source was heated to 130°C for approximately 15 minutes.



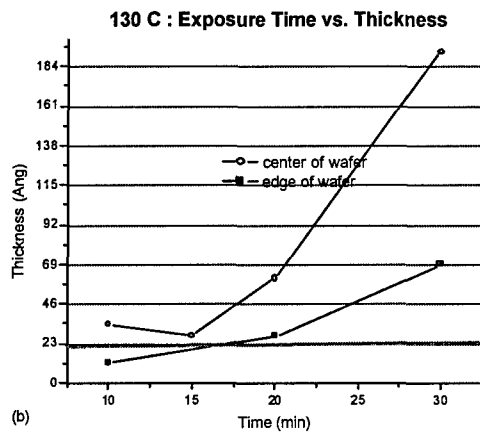
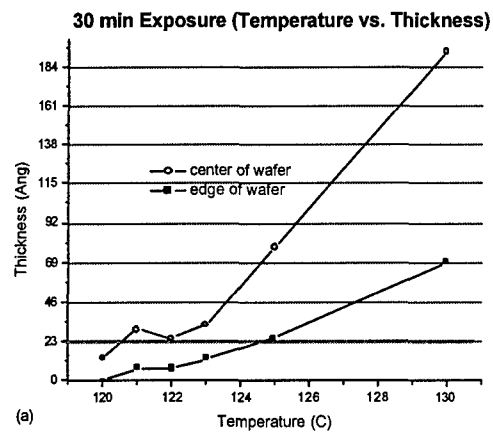


**Figure 3.2:** (a) Thickness vs. Temperature for samples exposed for 30 minutes, (b) Thickness vs. Time for samples exposed at a constant temperature of 130°C.

In order to investigate the composition of the films that were thicker than a monolayer (23Å), we rinsed the thicker films with tetrahydrofuran. Tetrahydrofuran (THF) is a solvent that should rinse away physisorbed alkanethiol molecules on gold, while leaving chemisorbed monolayers intact. The results for OPE films before and after rinsing are shown in Figures 3.3 (a) and (b) respectively. As one can see from the figure, the films had a variety of thicknesses prior to rinsing, but all were approximately 23 Å thick after rinsing. Thus, we confirmed that 23Å is the approximate thickness of a chemisorbed monolayer and that after a chemisorbed monolayer of molecules was assembled, additional molecules physisorbed on top of this initial monolayer.

If we were able to remove these physisorbed molecules in-situ, we could greatly widen the window of conditions required for a monolayer. Although we have shown that this can be done by rinsing the monolayers with THF, rinsing is not ideal for vapor phase processing. This is because rinsing the monolayers will negate some of the potential advantages of vapor phase deposition including: the possibility of performing all of the fabrication steps needed for devices in-situ (including metallization), and avoiding solvents that can contaminate the monolayers. We also attempted to remove the physisorbed molecules by heating the wafers to temperatures of approximately 130°C. However, this heating was performed with an existing sample heater and thermocouple, which were designed to only heat the sample reliably at

temperatures higher than 300°C. We were unable to use this heater to reproducibly heat the sample at such relatively low temperatures (even when we disconnected this heater from the thermocouple and controlled it manually). Thus, we determined that while heating the wafers to get rid of the physisorbed molecules may be possible, it would probably need to be done with a heater and thermocouple that were designed for such relatively low temperatures.

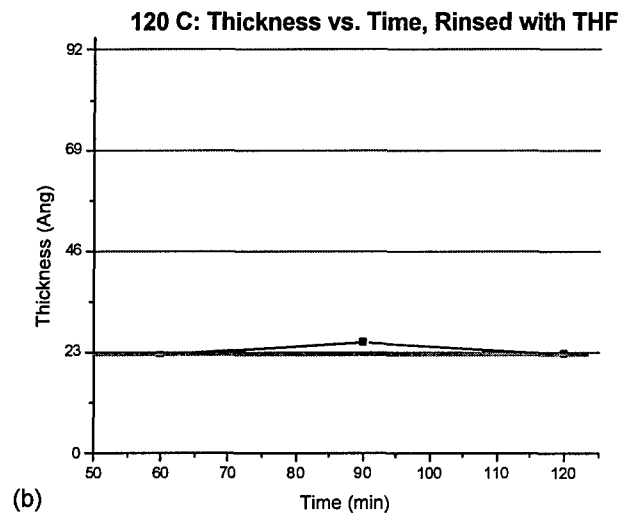
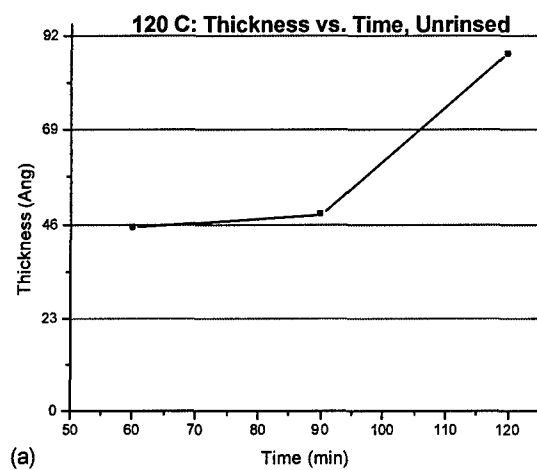


**Figure 3.3:** (a) OPE samples, unrinsed (b) OPE samples, rinsed with THF.

During the course of our experiments with OPEs, we reloaded the source crucible with more molecules. Although the molecular depositions that were performed before reloading the crucible were very reproducible, the deposition conditions had to be adjusted slightly after the crucible was reloaded with molecules. All of the results shown in Figure 3.2 are from a source crucible that was initially loaded with approximately 12mg of OPE molecules and was not reloaded in-between experimental runs. However, the crucible was reloaded with 20mg of molecules before doing the experimental runs that are shown in Figure 3.4 (Figure 3.4 shows film thicknesses for samples assembled at a source temperature of 120°C for a variety of exposure times). Comparing the thickness of the center of the wafer for a 30-minute exposure at 120°C from Figure 3.2 (a) of approximately 13Å with that from Figure 3.4 of approximately 30Å, one can see that the thickness between the two different crucible loads differs by more than 15Å. Thus, with each new loading of molecules, the conditions had to be changed slightly to achieve a monolayer of molecules (this may have been because the amount of molecules loaded into the crucible was different for the two loads). However, reestablishing the conditions for assembling exactly a monolayer of molecules after reloading the crucible was done in about one day and once established, the conditions were very reproducible from experimental run to experimental run.

120 C: Exposure Thickness vs. Time, 2nd source load

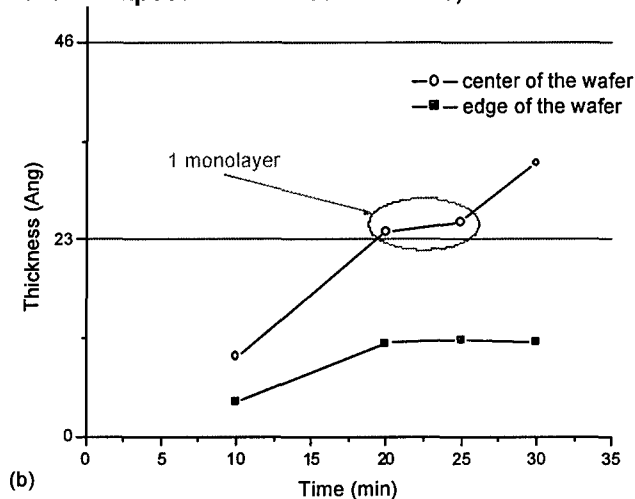


**Figure 3.4:** Thickness vs. exposure time for a constant source temperature of 120°C. This figure shows that the expected thickness for a monolayer (approximately 23Ang) was achieved for exposures of 20-25 minutes.

Once the conditions for the assembly of a monolayer of OPEs were established, they were reliable. We were able to assemble molecules on more than 30 samples without any change in the conditions required to achieve a monolayer. Figure 4 is an example of how by heating the source to 120°C for between 20 and 25 minutes, we could reproducibly achieve a film thickness of

approximately 24Å. We thus established a process window for consistently and reproducibly assembling a monolayer of OPE molecules. We next confirmed that the monolayers were uncontaminated, chemisorbed, and had regular structures (as described in the following sections).

## **XPS of OPE Molecules on Gold**

After assembling monolayers, we packed them in a nitrogen environment and shipped them to Rice University where X-ray photoelectron spectroscopy (XPS) was performed. The XPS of films that were less than 23 Å thick (as determined by ellipsometry) showed that all of the sulfur endgroups of the molecules were bound to gold, indicating that all of the molecules were chemisorbed to the gold surface (see Figure 3.5 (a)). However, the XPS of the films that were thicker than 23 Å showed peaks for bound sulfur as well as unbound sulfur endgroups (see Figure 3.5 (b)), indicating that the samples with a thickness greater than that expected for a single monolayer had both chemisorbed and physisorbed molecules. Thus, the samples with an ellipsometry thickness of 23 Å or less have a chemisorbed monolayer (although samples with a thickness less than 23 Å would have an incomplete monolayer). However, for the thicker samples, after the first monolayer is chemisorbed, the additional incoming molecules seem to pile up and physisorb on top of the chemisorbed monolayer. This confirms what rinsing the films with THF showed (see Figure 3.3). XPS also showed that the

monolayers were uncontaminated and thus verified that vapor phase deposition was a clean assembly method.

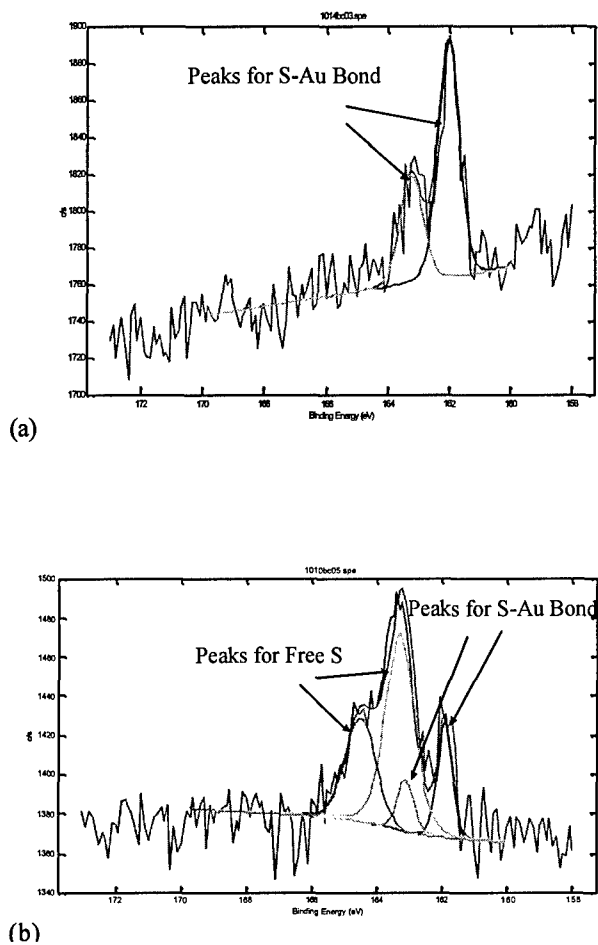


**Figure 3.5:** (a) XPS of a 23 Angstrom thick sample that showed bound sulfur peaks, (b) XPS of a sample thicker than 23 Angstroms that showed both the bound and the unbound sulfur peaks.



## STM of the OPE Molecules on Gold

Scanning tunneling microscopy (STM) was performed using a Molecular Imaging PicoPlus scanning probe microscope. All samples that were used for STM consisted of gold evaporated on 5nm of Ti (for adhesion) on a 500nm thick silicon dioxide layer on silicon. After the gold was evaporated and prior to the molecular assembly, these substrates were flame-annealed to enlarge grain sizes for improved imaging. The oxide layer between the bottom silicon and the Ti/Au layer acted as a barrier and reduced the migration of silicon during flame annealing.

When we imaged the deposited films with STM, samples that were 23 Angstroms or thicker showed ordering (see Figure 3.6). This ordering was indicative of a chemisorbed dense monolayer of molecules in the standing up phase<sup>25,26,27</sup>. However, similar ordering was also observed from samples with monolayers that ellipsometry indicated to be thicker or thinner than 23 Angstroms. This may be due to the fact the STM indicates local ordering, whereas ellipsometry averages monolayer density of relatively larger areas.

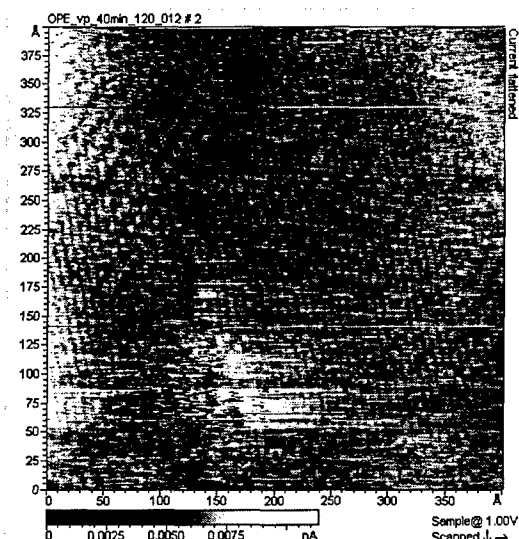


**Figure 3.6:** STM image of a sample of OPE molecules on gold using a Molecular Imaging PicoPlus with Pt/Ir tip, "striping" in image is indicative of ordering of the monolayer.

### Electrical Results from OPEs Assembled in the Nanowell Device via Vapor Phase Deposition

After establishing that vapor phase deposition could be used to grow OPE molecules on gold wafers and achieve the dense standing up layer, a similar procedure was used to deposit molecules in nanowell devices. The nanowell devices were made using a new crossbar architecture that consisted of gold lines (or "bars") that were 10  $\mu\text{m}$  wide, covered with 100nm of nitride, and then with photoresist, which was developed to expose the lines for the top gold "bars". Next, 100nm wells were milled through the nitride at each wire junction using

focused ion beam (FIB). The chips were then cleaned with a piranha etch (sulfuric acid and hydrogen peroxide in a ratio of 3:1), loaded into a tantalum chip holder, and then loaded into the FEL. The same procedure for vaporizing OPE molecules was followed as described in section 3.3. After the chips were removed, gold was deposited and liftoff was performed to form the top bars of the crossbar device. This crossbar structure is shown below in Figure 3.7.

### Optical Micrograph of Crossbar

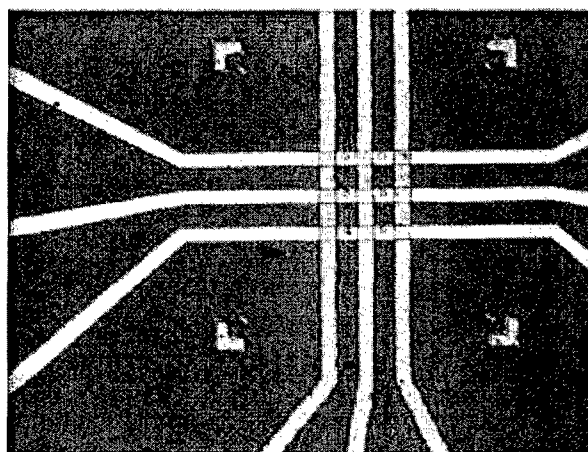


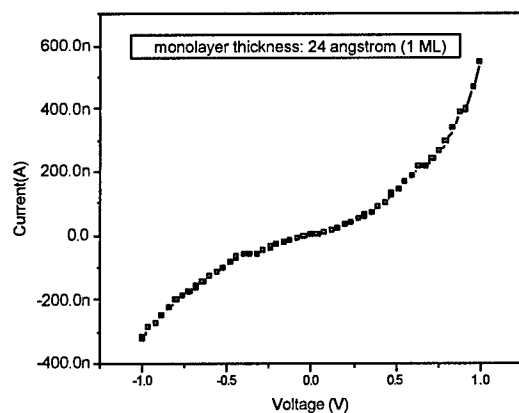
Figure 3.7: The crossbar structure.

We used the crossbar structure architecture for our nanowell devices for two reasons. Firstly, we had used all of the pre-patterned chips that had been previously fabricated at MCNC. Secondly, with the crossbar structure, devices

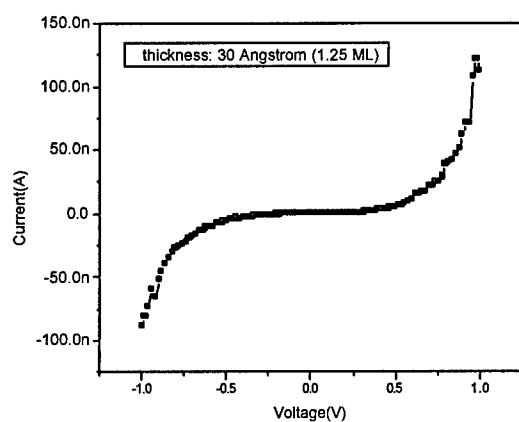
could be tested in series and/or parallel to further investigate the molecular electrical device characteristics.

We were unable to fabricate this crossbar structure prior to the development of the vapor phase deposition procedures. This was because the solvents used in solution phase would rinse away the photoresist required to pattern the top gold "bars". Thus, after vapor phase deposition was established as effective, it was used as the exclusive method for fabricating nanowell crossbar architectures.

After the crossbar nanowell devices were fabricated, they were electrically characterized. Figure 3.8 (a) shows the I-V curve for a device that had an OPE monolayer assembled. As one can see, these electrical results are qualitatively similar to those for nanowell devices fabricated using solution phase assembly. It was not possible to compare the yields of solution phase and vapor phase deposition of the OPE since all vapor phase deposition was performed using the crossbar architecture and all solution phase was performed using the original pre-patterned single device chips.



(a)



(b)

**Figure 3.8:** (a) The I-V characteristics of a crossbar nanowell device with a single monolayer of molecules assembled, (b) the I-V characteristics of a crossbar nanowell device with more than a monolayer of molecules assembled.

When the nanowell crossbar device was fabricated with a film of OPEs that was thicker than a monolayer, the electrical characteristics were qualitatively different from those with exactly a monolayer (see Figure 3.9 (a), (b)). This indicates that the electron transport switches from being that of "through-bond" tunneling (as is the case with the monolayer of OPEs) to a combination of quantum mechanical tunneling and through-bond tunneling for the thicker film. Additionally, the differing results exemplify how a device's electrical characteristics depend on the structure and thickness of the film. This could provide insight into why different research groups have observed different electrical results when testing the same molecules: the quality of the monolayer affects the electrical results.

## Summary

We were able to establish the conditions for using vapor phase deposition to reproducibly assemble a single monolayer of dense, chemisorbed, uncontaminated OPE molecules. Establishing vapor phase deposition enabled us to fabricate nanowell devices in a crossbar architecture. We found that the electrical results for a device with a film one monolayer thick were qualitatively similar to devices we fabricated from solution phase. However, devices with films thicker than a monolayer showed electrical characteristics that differed from those with exactly a monolayer. This exemplifies the need for the ability to

controllably deposit monolayers of molecules. Vapor phase deposition not only provided us with the ability to controllably deposit an ordered monolayer, but also enabled us to fabricate more complex structures such as the crossbar.

## 7.6 Works Cited for This Section

1. C. Zhou et al, *Appl. Phys. Lett.* **71**, 611 (1997).
2. M. A. Reed et al, *Appl. Phys. Lett.* **78**, 3735 (2001).
3. I. Kratochvilova et al, *Journal of Materials Chemistry* **12**, 2927 (2002).
4. F. F. Fan et al, *J. Am. Chem. Soc* **124**, 5550 (2002).
5. Z. J. Donhauser et al, *Science* **292**, 2303 (2001).
6. P. A. Lewis et al, *J. Am. Chem. Soc.* **126**, 12214 (2004).
7. J. Chen et al, *Science* **286**, 1550 (1999).
8. C. Li et al, *Appl. Phys. Lett.* **82**, 645 (2003).
9. D. J. Wold, C. D. Frisbie, *J. Am. Chem. Soc.* **123**, 5549 (2001).
10. L. A. Bumm et al, *Science* **271**, 1705 (1996).
11. X. D. Cui et al, *Nanotechnology* **13**, 5 (2002).
12. R. P. Andres et al, *Science* **272**, 1323 (1996).
13. M. A. Reed et al, *Science* **278**, 252 (1997).
14. I. Kratochvilova et al, *J. Mater. Chem.* **12**, 2927 (2002).
15. I. Smlsni et al, *Appl. Phys. Lett.* **80**, 2761 (2002).
16. J. G. Kushmerick et al, *Phys. Rev. Lett.* **89**, 086802 (2002).
17. Y. Luo et al, *Chem. Phys. Chem.* **3**, 519 (2002).
18. W. Wang et al, *Supperlattices and Microstructures* **33**, 217 (2003).
19. N. Gergel et al, *J. Vac. Sci. Technol. A.* **23** (4), 880 (2005).
20. D. L. Pugmire et al, *Langmuir* **19**, 3720 (2003).
21. T. Nakamura et al, *Langmuir* **12**, 5977 (1996).

Formatted: Bullets and Numbering



22. J. Lee et al, *Nano Letters* **3** (2), 113 (2003).
23. J.M. Tour et al, *Chem. Eur. J.* **7**, 5118, (2001).
24. C.T. Cai et al, *J. Phys. Chem B* **108**, 2827 (2004).
25. H. Kondoh et al, *Journal of Chemical Physics* **11** (3), 1175 (1999)).
26. G.E. Poirier et al, *Langmuir* **15**, 1167 (1999).
27. J.J. Stapleton et al, *Langmuir* **19**, 8245 (2003).